

CONTROL OF LASER RADIATION PARAMETERS

PACS numbers: 42.55.Wd; 42.60.Fc; 81.05.U–; 78.67.Ch
DOI: 10.1070/QE2013v043n08ABEH015027

Control over the performance characteristics of a passively mode-locked erbium-doped fibre ring laser

M.A. Chernysheva, A.A. Krylov, A.A. Ogleznev, N.R. Arutyunyan, A.S. Pozharov, E.D. Obraztsova, E.M. Dianov

Abstract. **We report an all-fibre ultrashort pulse erbium-doped ring laser passively mode-locked by single-wall carbon nanotubes dispersed in carboxymethylcellulose-based polymer films. Owing to intracavity dispersion management and controlled absorption in the polymer films, the laser is capable of generating both femto- and picosecond pulses of various shapes in the spectral range 1.53–1.56 μm. We have demonstrated and investigated the generation of almost transform-limited, inversely modified solitons at a high normal cavity dispersion.**

Keywords: *erbium-doped fibre laser, mode locking, group velocity dispersion compensation, carbon nanostructures, soliton.*

1. Introduction

Passively mode-locked fibre laser sources of ultrashort pulses (USPs) are widely used in many scientific and technological applications owing to their compact design, reliability and efficiency. At the same time, extremely important issues are a search for and characterisation of new laser operation modes that would allow one to improve characteristics of pulses, namely, to increase their energy, reduce their duration and improve their stability [1].

For these purposes, wide use is made of intracavity group velocity dispersion (GVD) management, which allows laser operation to be effectively controlled by incorporating positive and negative GVD components into the laser cavity [2]. This, in turn, influences the dynamics of pulses propagating through the cavity and, as a consequence, other output characteristics of the laser [3]. In particular, Im et al. [4] used a normal dispersion fibre segment to control the GVD in an erbium-doped fibre laser, which is generally accepted in the 1.55-μm spectral region. The evolution of generated pulses in response to variations in cavity dispersion and changes in radiative losses in an erbium-doped fibre ring laser was described by Nishizawa et al. [5]. At the same time, the pulse generation process in a cavity is strongly influenced not only by the net GVD but also by the nonlinearity of the fibres, the relationship between saturable and nonsaturable losses in the cavity and the pump power.

In earlier studies, passive mode locking of fibre lasers was achieved using modulators based on Kerr nonlinearity [1, 2] and semiconductor saturable absorber mirrors (SESAMs) [1, 6].

After single-wall carbon nanotubes (SWCNTs) were first used in 2003 as saturable absorbers for passive mode locking [7], they have been employed increasingly in advanced USP lasers. SWCNT-based saturable absorbers offer an ultrashort excited-state relaxation time (shorter than ~500 fs) [8] and strong nonlinear absorption modulation, are relatively easy to fabricate and can be incorporated into various laser configurations rather readily [9].

A unique feature of SWCNTs is that the density of electronic states in them and their band gap depend on the tube diameter. The possibility of tuning the band gap of SWCNTs by varying their diameter or chirality indices [10] and the fast relaxation of electronic excitations in them allow one to use them as saturable absorbers in a wide spectral range [11]. The most widespread approach for incorporating SWCNTs into a fibre laser configuration is through dispersing the nanotubes in polymer films [9] possessing good homogeneity and high optical quality, which are then clamped between fibre end faces [9, 12].

In this paper, we report an erbium-doped fibre ring laser passively mode-locked by SWCNTs dispersed in carboxymethylcellulose-based polymer films, with intracavity GVD management through the incorporation of a highly nonlinear low-loss single-mode germanosilicate fibre with a high normal GVD in the spectral range 1.53–1.56 μm. We have studied in detail the influence of the cavity dispersion and the transmittance of the SWCNT-containing polymer films on the duration and spectrum of the resulting pulses.

2. Experimental setup

Figure 1 shows the erbium-doped fibre ring laser configuration. The gain medium of the laser was a 1.2-m length of a step-index (Δn = 0.005) erbium-doped aluminosilicate fibre (core diameter $d \approx 10$ μm) with an unsaturated absorption of 11 dB m^{-1} at the pump wavelength (980 nm). The active fibre was pumped by a laser diode with up to 200 mW of output power through a fibre multiplexer which combined signals at 0.98 and 1.55 μm in the fibre core.

The saturable absorbers used to ensure passively mode-locked laser operation were polymer films containing SWCNTs. A film was fixed between the ferrules of two APC/FC fibre connectors (Fig. 1), which were angle-polished at 7° to minimise back reflection. In the literature, such a module containing an SWCNT film is referred to as a saturable absorber incorpo-

M.A. Chernysheva, A.A. Krylov, E.M. Dianov Fiber Optics Research Center, Russian Academy of Sciences, ul. Vavilova 38, 119333 Moscow, Russia; e-mail: sokolak@mail.ru;
A.A. Ogleznev Perm Research and Production Instrument Company, ul. 25 Oktyabrya 106, 614990 Perm, Russia;
N.R. Arutyunyan, A.S. Pozharov, E.D. Obraztsova A.M. Prokhorov General Physics Institute, Russian Academy of Sciences, ul. Vavilova 38, 119991 Moscow, Russia; e-mail: elobr@kapella.gpi.ru

Received 19 October 2012; revision received 19 February 2013
Kvantovaya Elektronika **43** (8) 691–698 (2013)
Translated by O.M. Tsarev

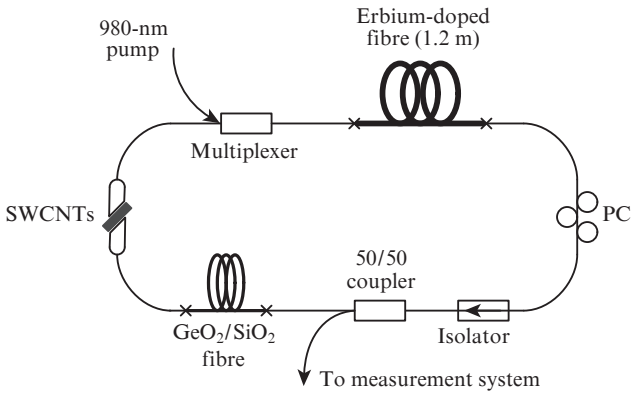

Figure 1. Schematic of the erbium-doped fibre ring laser with intracavity GVD management.

rating nanotubes (SAINT) [9, 12]. In addition, unidirectional lasing in the ring was ensured by an optical isolator with SMF-28 isotropic fibre pigtails.

The laser output was decoupled from the cavity by a 50/50 coupler. It is worth pointing out that the fraction of light decoupled from the fibre and the position of the coupler in the cavity were adjusted so as to maximise the laser efficiency and, at the same time, to reduce the intensity incident on the SWCNT-containing film, thereby reducing the radiation exposure of the film. As a result, the coupler was placed before the SWCNT module, which ensured an appreciable increase in permissible output power.

One of the most important components of the laser is a fibre polarisation controller (PC). Accurate adjustment of the PC ensures stable passively mode-locked laser operation in a single-pulse mode and, as shown below, makes it possible in some cases to control laser pulse characteristics.

Intracavity GVD management was ensured by varying the length of a highly nonlinear germanosilicate (GeO_2/SiO_2) fibre with a normal dispersion of –170 ps nm^{-1} km^{-1} at a wavelength of 1.56 μm, which was inserted in the cavity to compensate for the anomalous dispersion introduced by the erbium-doped and (passive) SMF-28 fibres (the multiplexer, coupler and polarisation controller were made from SMF-28). Those fibres were similar in GVD: 19 and 16.5 ps nm^{-1} km^{-1}, respectively. The core of the GeO_2/SiO_2 fibre contained 75 mol% germania and its diameter was less than 2 μm ($\Delta n \approx 0.11$). Its second-order mode cutoff wavelength was measured to be $\lambda_{cr} \approx$ 970 nm [13]. The nonlinearity coefficient of the GeO_2/SiO_2 fibre was estimated at $\gamma_{Ge} \approx 30$ W^{-1} km^{-1}, which exceeds those of the erbium-doped fibre and SMF-28 ($\gamma_{SMF} \approx 1$ W^{-1} km^{-1}) by one and half orders of magnitude.

Single-wall carbon nanotubes were produced by arc discharge between graphite electrodes in a helium atmosphere, using nickel and yttria as catalysts ($C:Ni:Y_2O_3 = 2:1:1$) [14]. It is worth noting that the arc discharge method was chosen because the absorption band of SWCNTs prepared by this method is shifted to the IR [15] relative to that of SWCNTs produced by other methods, e.g. by high-pressure gas-phase carbon monoxide (CO) decomposition catalysed by Fe particles (referred to as the HiPCO process in the literature), laser ablation or chemical vapour deposition (CVD). The method chosen by us improves the efficiency of SWCNTs as saturable absorbers in rare-earth-doped fibre lasers.

The main polymer for film production was carboxymethylcellulose (CMC), which is a good surfactant and has a matrix structure. This allows one to produce SWCNT-containing films of high optical quality without using other polymers. In addition, CMC is a sufficiently flexible material, which allows films down to 4 μm in thickness to be produced [16].

Stable SWCNT suspensions were prepared by dispersing arc-discharge soot in an aqueous 1 wt% CMC solution through sonication, followed by ultracentrifugation at $1.5\times10^5 g$. The resultant homogeneous solution had the form of a suspension of individual SWCNTs and was used to prepare films [17]. The quality of the polymer films was assessed using Raman spectroscopy [18] and optical absorption measurements in a wide spectral range. The diameter of the synthesised SWCNTs was estimated at about 14 Å from their Raman spectra.

In examining the dynamics of laser characteristics (in particular, their response to changes in optical losses), we varied the thickness of the polymer films and the concentration of SWCNTs dispersed in the films.

We studied relatively thick (25–30 μm), opaque films (samples 1 and 2), which had an unsaturated absorption of 67% in the range 1.53–1.56 μm, and a more transparent film (sample 3), about 15 μm thick, with a considerably weaker absorption (about 30%). It is worth noting that the most stable passively mode-locked laser operation was observed when two films were used simultaneously. The total absorption was then 39% for sample 3 and about 86% for samples 1 and 2. The unsaturated IR absorption spectra of the SWCNT-containing polymer films are presented in Fig. 2.

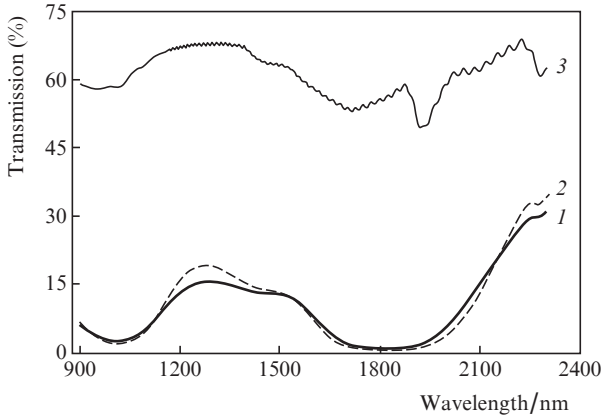

Figure 2. Transmission spectra of pairs of SWCNT-containing polymer films. Spectra *1–3* refer to samples 1–3, respectively.

3. Results and discussion

We achieved stable passively mode-locked single-pulse laser operation with an insignificant pulse amplitude modulation (less than 2%) even over long time intervals (up to 1 ms).

In our experiments, the germanosilicate fibre was cut back starting at 1.2 m, which corresponded to a variation in net cavity GVD from +0.194 to –0.068 ps^2. As a result, the pulse repetition rate was varied from 42 to 57 MHz. Figure 3 illustrates the effect of cavity GVD on the key laser characteristics: the pulse intensity autocorrelation trace (ACT) width, $\Delta\tau_a$; the full width at half maximum (FWHM) of the emission band, $\Delta\lambda$; and the time–bandwidth product C ($C = \Delta\nu\Delta t_p$, where $\Delta\nu$ is the FWHM of the pulse in frequency space and Δt_p is the pulse duration).

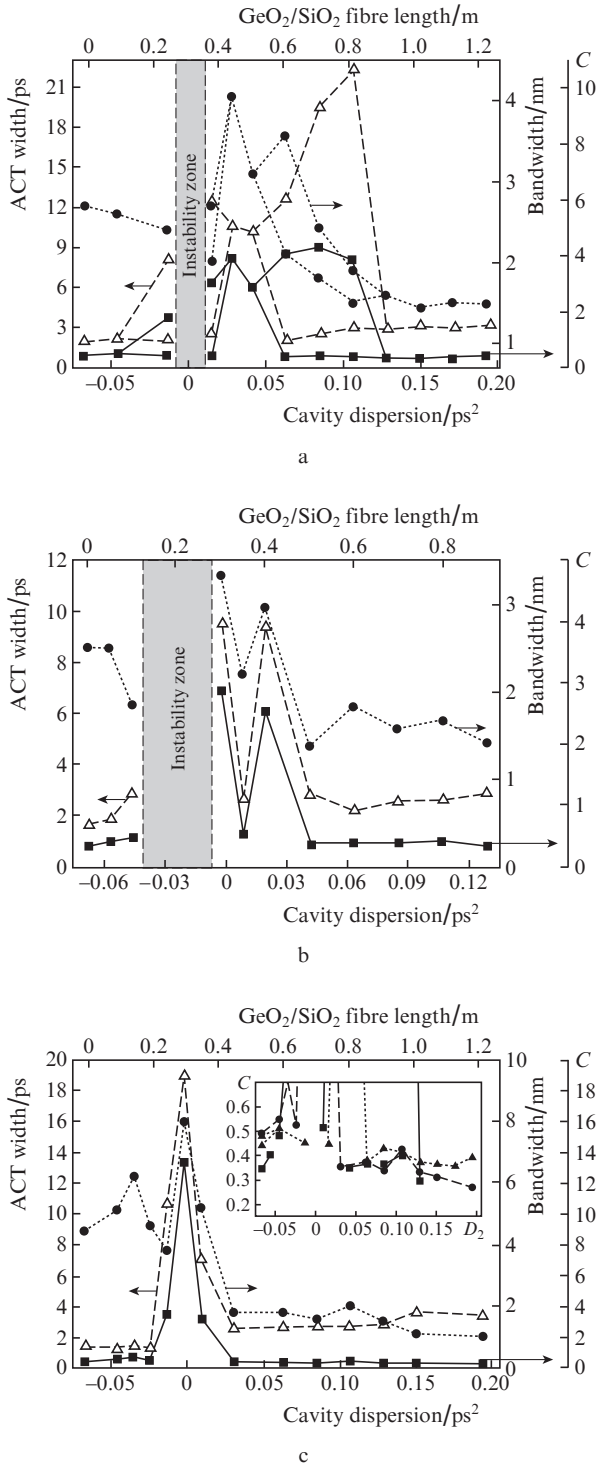

Figure 3. Effect of cavity GVD on output laser pulse characteristics for samples (a) 1, (b) 2 and (c) 3. Inset: variation in the time–bandwidth product C of samples 1 (▲), 2 (■) and 3 (●).

It should be especially emphasised that, in the case of the opaque films (samples 1 and 2), we observed suppression of mode locking at a near-zero cavity GVD and a transition to chaotic pulse generation (Figs 3a, 3b). By contrast, the laser containing sample 3 had no unstable mode locking region (Fig. 3c). Moreover, varying the unsaturated absorption in the films and the GVD in the cavity had a significant effect on the pulsed lasing threshold and the highest output power in a single-pulse mode.

Reducing the germanosilicate fibre length from 25 cm to zero corresponds to a change in net anomalous cavity GVD from –0.024 to –0.068 ps^2, which suggests optical soliton generation [2]. Indeed, using SWCNT-containing films differing in absorption, we identified soliton-like pulses. The centre emission wavelength of the laser containing films 1 and 2 almost coincided with the peak gain wavelength of the erbium-doped aluminosilicate fibre (about 1.53 μm [19]). The emission spectra in Fig. 4a are very similar and have a bandwidth of 2.7 and 3.1 nm, with an average power of 2.1 and 3 mW, respectively. The laser containing the transparent SWCNT film (sample 3) has a longer peak emission wavelength (1.56 μm), and its emission band is markedly broader, reaching 6.5 nm in the middle of the indicated dispersion interval (D_2 = –0.035 ps^2) and decreasing to about 4.5 nm at its boundaries.

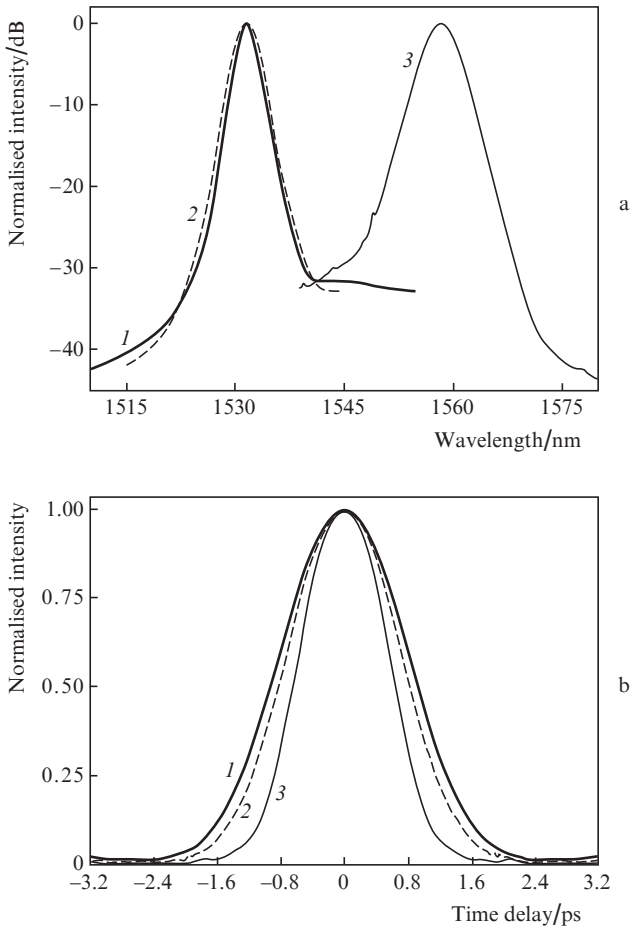

Figure 4. (a) Emission spectra and (b) corresponding pulse intensity ACTs at a cavity dispersion D_2 = –0.068 ps^2: (*1*) sample 1, pulse duration $\Delta t_p \approx 1.2$ ps, full width at half maximum of the emission band $\Delta\lambda = 2.7$ nm, average output power $P_{out} = 2.14$ mW; (*2*) sample 2, $\Delta t_p \approx 1.08$ ps, $\Delta\lambda = 3.1$ nm, $P_{out} = 3.04$ mW; (*3*) sample 3, $\Delta t_p \approx 790$ fs, $\Delta\lambda = 4.48$ nm, $P_{out} = 3.33$ mW.

The pulse intensity ACTs of this laser are sufficiently well represented by a curve corresponding to a soliton [20], as illustrated in Fig. 5a. When there is no germanosilicate fibre (at D_2 = –0.068 ps^2), the ACTs of pulses generated by the lasers containing films 1, 2 and 3 are 1.85, 1.67 and 1.22 ps in width, respectively (Fig. 4a). From these data, the soliton-like pulse duration was estimated at 1.2, 1.08 and 0.79 ps, respectively.

The considerable increase in losses in lasers containing opaque SWCNT films requires an increased population inversion level in their gain medium, which leads to a marked narrowing of the peak in the gain curve of erbium-doped aluminosilicate fibre near 1.53 μm [19]. The gain medium then acts as a filter that limits the spectral band of the light in the cavity. It is this effect which is responsible for the marked narrowing of the emission spectrum of the laser containing (opaque) films 1 and 2. The emission spectrum of a laser can be shifted to longer wavelengths either by reducing the cavity loss, as illustrated by the present results, or by increasing the active fibre length, thereby shifting the integrated gain peak of the fibre to longer wavelengths. It should be noted that further varying the cavity GVD has no effect on the position of the emission band when appropriate SWCNT-containing films are used.

Increasing the average output power of the laser reduces the pulse duration and, accordingly, increases the laser emission bandwidth (Fig. 5). This correlates with the fact that the soliton duration is inversely related to the soliton energy, $\Delta t_s \sim 1/E_s$ [2], which also points to soliton generation in the case of anomalous net cavity GVD. In addition, the spectra presented in Fig. 5b contain well-defined Kelly sidebands, characteristic of soliton lasers [21]. The shortest soliton duration was 675 fs.

At a near-zero cavity GVD, the laser generates picosecond pulses with an almost rectangular spectrum (on a logarithmic scale). Under these conditions, the duration of pulses with a Gaussian envelope ranges from 6.5 to 8.5 ps in the lasers containing films 1 and 2 and reaches 13 ps in the case of sample 3 (Fig. 6a). The corresponding spectra are almost identical in shape, with sharp edges (Fig. 6b), but their –10 dB bandwidth is about 3 nm in the case of samples 1 and 2 and reaches 8.4 nm in the laser containing sample 3. Therefore, the time–bandwidth product C, which is 3, 2.9 and 13.4 for samples 1, 2 and 3, respectively, considerably exceeds the $C_0 = 0.441$ of a transform-limited Gaussian pulse, indicating an appreciable pulse phase modulation (chirp). The linear chirp $\alpha = (\partial^2\varphi/\partial t^2)t_0^2$ in dimensionless form (i.e. normalised to the square of the inverse pulse duration) can be estimated using the relation [22]

$$\alpha \approx [(C/C_0)^2 - 1]^{1/2}, \quad (1)$$

which gives $\alpha \approx 30$ for a pulse corresponding to curve (*3*) in Fig. 6. Thus, the pulse is highly chirped and can be compressed to femtosecond durations using an appropriate external dispersion delay line [22].

Like in the case of soliton generation, spectral filtration in a highly inverted gain medium near 1.53 μm reduces the

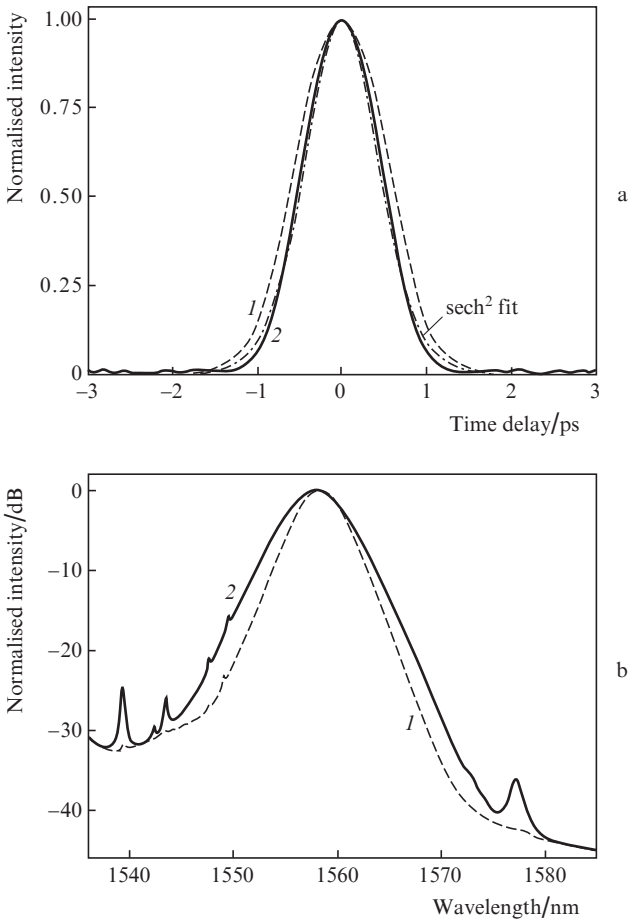

Figure 5. (a) Pulse intensity ACTs and (b) corresponding emission spectra of the laser containing film 3 at a cavity dispersion $D_2 = -0.068$ ps^2: (*1*) $\Delta t_p \approx 790$ fs, $\Delta\lambda = 4.48$ nm, $P_{out} = 3.33$ mW; (*2*) $\Delta t_p \approx 675$ fs, $\Delta\lambda = 5$ nm, $P_{out} = 4.41$ mW. The dot-dashed line represents a fit with a soliton ACT [20].

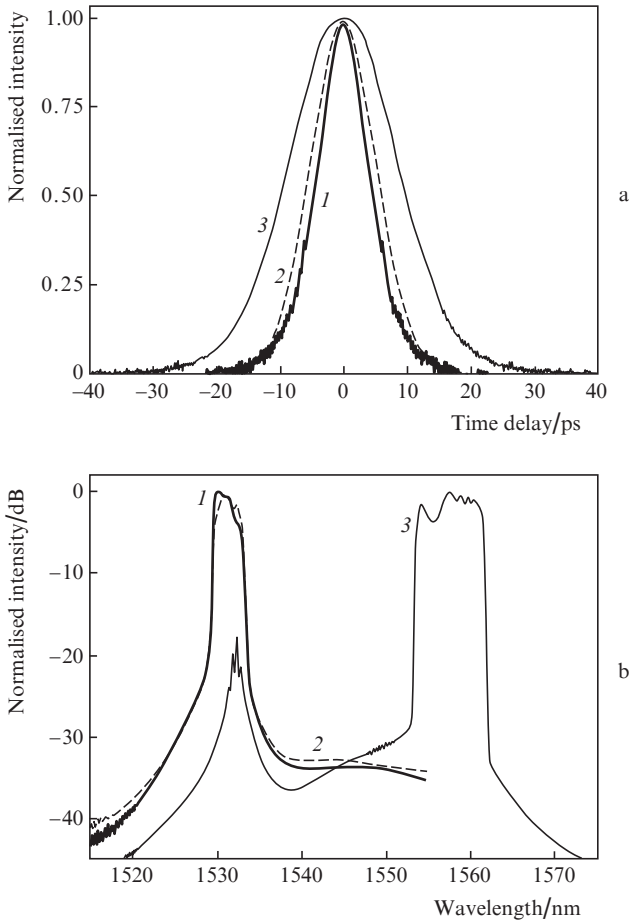

Figure 6. (a) Pulse intensity ACTs and (b) corresponding emission spectra at a near-zero cavity GVD for samples (*1*) 1 ($D_2 \approx -0.002$ ps^2, $\Delta t_p \approx 6.77$ ps, $\Delta\lambda = 3.33$ nm, $C = 2.88$, $P_{out} = 2.8$ mW), (*2*) 2 ($D_2 \approx +0.015$ ps^2, $\Delta t_p \approx 8.56$ ps, $\Delta\lambda = 2.71$ nm, $C = 3.02$, $P_{out} = 5$ mW) and (*3*) 3 ($D_2 \approx -0.002$ ps^2, $\Delta t_p \approx 13$ ps, $\Delta\lambda = 8.38$ nm, $C = 13.4$, $P_{out} = 10.5$ mW).

emission bandwidth of the lasers based on the opaque SWCNT-containing films by more than a factor of 2.

Increasing the pump power increases the pulse duration, whereas the emission bandwidth varies only slightly.

It is important to note that, at a near-zero cavity GVD, we failed to detect generation of pulses whose duration would oscillate ('breathe') during propagation through normal and anomalous GVD fibres (stretched-pulse generation) [2]. Instead, the generation of chirped pulses with a rectangular spectrum was demonstrated. We believe that this atypical behaviour of the laser system is mainly due to the use of the highly nonlinear germanosilicate fibre for intracavity GVD management. Indeed, in the stretched-pulse regime, the evolution of pulses in fibres with opposite signs of GVD is expected to be absolutely symmetric [2]. In the case under consideration, however, the use of the highly nonlinear GeO_2/SiO_2 fibre, which introduces high normal dispersion, considerably distorts the symmetry in the ring, preventing large pulse duration oscillations. Highly chirped pulses with a rectangular spectrum are typically generated by lasers with a high normal cavity GVD [4, 5], but the presence of highly nonlinear germanosilicate fibre radically changes laser operation in the zero dispersion region.

Indeed, the cavity-average dispersion length (L_D) and nonlinear length (L_{NL}) for a pulse with a Gaussian envelope of duration Δt_p can be estimated as

$$L_D = \frac{\Delta t_p^2 L_{res}}{4 \ln 2 \, |D_2|}, \; L_{NL} = \frac{\Delta t_p f}{\gamma_{Ge} P_{av}} \frac{L_{res}}{L_{Ge}}, \qquad (2)$$

were L_{res} is the resonator length; L_{Ge} is the GeO_2/SiO_2 fibre length; D_2 is the net cavity GVD; f is the pulse repetition frequency; and P_{av} is the average optical power coupled into the GeO_2/SiO_2 fibre. Estimates for a pulse corresponding to curve (*3*) in Fig. 6 (sample 3, L_{res} = 4 m, f = 50.4 MHz, L_{Ge} = 24 cm, P_{av} = 10.5 mW) give $L_D \sim 1.2 \times 10^5$ m and $L_{NL} \sim 35$ m, i.e. the condition $L_D, L_{NL} \gg L_{res}$ is fulfilled. Therefore, the relationship between the nonlinear and dispersion lengths is $N = (L_D/L_{NL})^{1/2} \sim 60$. Clearly, at pulse durations of ~10 ps, the influence of both the normal and anomalous dispersions in each cavity segment is considerably weaker than that of nonlinearity, especially when the pulse propagates through the highly nonlinear GeO_2/SiO_2 fibre. The largest round-trip phase shift caused by self-phase modulation (SPM) can be estimated as $\phi_{NL} = L_{res}/L_{NL} = 0.036\pi$, i.e. $\phi_{NL} \ll \pi$. The low ϕ_{NL} value indicates that the spectrum of the pulses experiences insignificant round-trip SPM-induced distortion, so that pulse phase modulation remains almost linear [23]. This, in turn, allows one to increase the pulse energy while maintaining stable single-pulse laser operation, which is characteristic of lasers that generate dissipative solitons [4, 5, 23].

In the process of USP formation from a long Q-switching pulse, its compression in the initial stage occurs mainly when it passes through a saturable absorber (SWCNT-containing films in our case) [24]. At the same time, when the pulse duration decreases and the pulse intensity rises, the influence of SPM and GVD in the fibre becomes significant [2, 24]. In the case under consideration, their influence is, however, insufficient for further pulse compression or stretched-pulse generation in the cavity. The self-consistency principle for USP propagation through a cavity leads us to assume that a chirped pulse is compressed in the saturable absorber and in the neighbouring anomalous GVD fibre segment and is then again stretched in the GeO_2/SiO_2 fibre owing to its large normal dispersion, with a minimum in pulse duration at the boundary between the anomalous and normal GVD regions [23].

The laser containing sample 1 exhibited an interesting feature at GVD values between –0.02 and +0.13 ps^2. Varying the polarisation state of light in the cavity, we identified two types of pulses differing drastically in spectral shape (Fig. 7a). One type of pulse had a rectangular shape, whereas the other was nearly triangular in shape (on a logarithmic scale). Their intensity ACTs (Fig. 7b) differed in width by almost one order of magnitude, their durations were 8.9 and 1.4 ps, and their spectral widths were 3.57 and 2.12 nm, respectively. This feature of laser operation attests to a strong influence of polarisation effects when a pulse circulates in the ring, that is, to a significant polarisation sensitivity of the passive mode-locking regime. The polarisation sensitivity of the cavity can be contributed as well by the SWCNT-containing films, which requires, however, further investigation.

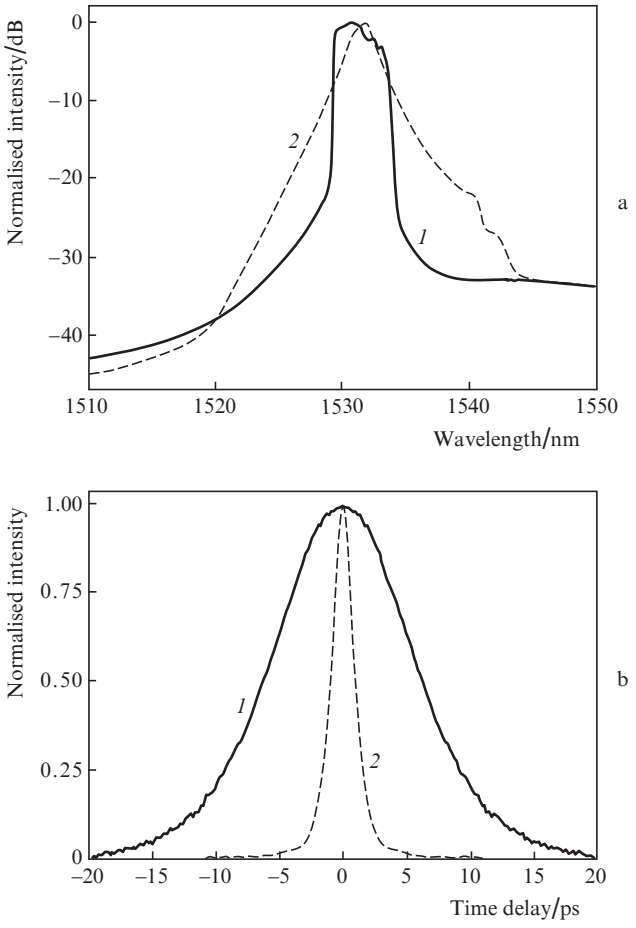

Figure 7. (a) Emission spectra and (b) corresponding pulse intensity ACTs of the laser containing sample 1 for different states of the polarisation controller: (*1*) $D_2 \approx +0.063$ ps^2, $\Delta t_p \approx 8.9$ ps, $\Delta\lambda = 3.57$ nm, $C = 4.07$, $P_{out} = 3.14$ mW; (*2*) $D_2 \approx +0.063$ ps^2, $\Delta t_p \approx 1.4$ ps, $\Delta\lambda = 2.12$ nm, $C = 0.37$, $P_{out} = 3.21$ mW.

In the essentially normal cavity GVD region, we observe the generation of stable pulses with an intensity ACT width oscillating around 3 ps (Fig. 3). Their emission bandwidth lies in the range 1–2 nm in the laser containing films 1 and 3 and in the range 1.5–2.5 nm in the laser containing sample 2, with an average output power of 1–6 mW. The spectra and intensity ACTs of pulses at $D_2 = +0.129$ ps^2 are presented in Fig. 8.

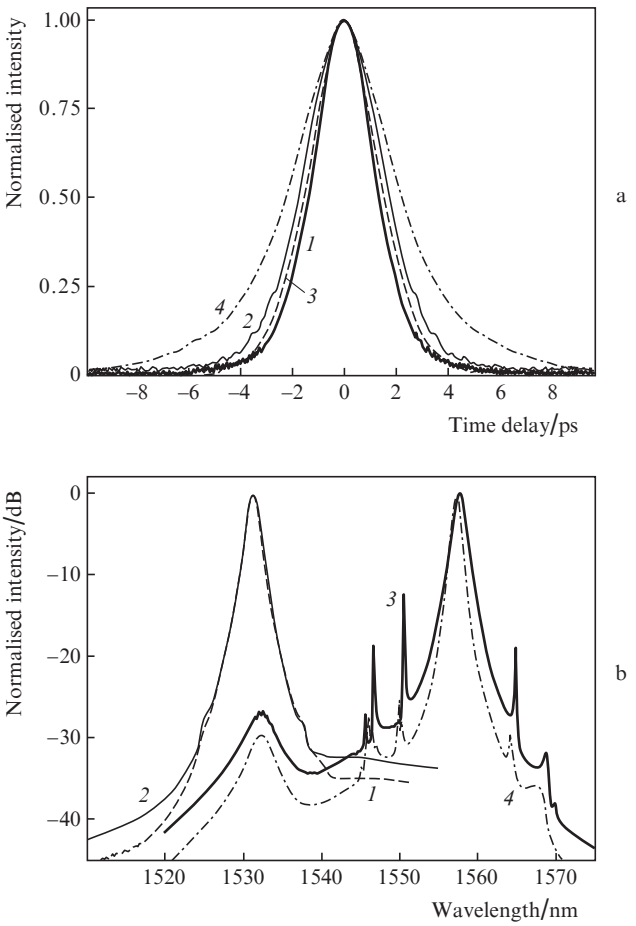

Figure 8. (a) Pulse intensity ACTs and (b) corresponding emission spectra at $D_2 = +0.129$ ps^2: (*1*) sample 1 ($\Delta t_p \approx 1.54$ ps, $\Delta\lambda = 1.42$ nm, $C = 0.32$, $P_{out} = 2.86$ mW), (*2*) sample 2 ($\Delta t_p \approx 1.82$ ps, $\Delta\lambda = 1.62$ nm, $C = 0.39$, $P_{out} = 1.7$ mW), (*3*) sample 3 ($\Delta t_p \approx 1.78$ ps, $\Delta\lambda = 1.39$ nm, $C = 0.31$, $P_{out} = 1.84$ mW), (*4*) sample 3 ($\Delta t_p \approx 2.68$ ps, $\Delta\lambda = 0.9$ nm, $C = 0.28$, $P_{out} = 3$ mW).

Note that, in the case of film 3, the emission spectrum contains sidebands. Even though these features are visually similar to Kelly peaks [21] in the spectra of soliton lasers, we cannot assert that there is soliton generation because the laser cavity has essentially normal GVD. Moreover, the position of the peaks relative to the centre wavelength of the laser is independent of pulse energy.

The variation of the pulse duration with energy is, in turn, completely opposite to soliton-like behaviour, with direct, rather than inverse, proportionality. In particular, increasing the average output power of the laser containing sample 3 from 1.84 to 3 mW increased the pulse intensity ACT width from 2.8 to 4.2 ps, whereas the emission bandwidth decreased from 1.5 to 1 nm [Fig. 8, curve (*4*)].

On the other hand, the time–bandwidth product C was considerably smaller than that of Gaussian pulses (0.441). It was about 0.3 and depended on the GVD, the transmission of the SWCNT films and the pulse energy. Fitting the emission spectrum with a Gaussian yielded a considerable discrepancy in the wings, as illustrated in Fig. 9a.

The temporal profile $I(t)$, spectral dependence $I(\omega)$ and intensity ACT $G_2(\tau)$ of the pulses obtained [20] were represented by

$$I(t) = \{\exp[7t/(4T_0)] + \exp(-4t/T_0)\}^{-2}, \quad (3)$$

$$I(\omega) = \left(1 - \frac{1}{\sqrt{2}}\right)\left[\cosh\frac{7\pi}{16}(\omega T_0) - \frac{1}{\sqrt{2}}\right]^{-1}, \quad (4)$$

$$G_2(\tau) = \left[2\cosh\left(\frac{16}{7}\frac{\tau}{T_0}\right) + 3\right]\left[5\cosh^3\left(\frac{8}{7}\frac{\tau}{T_0}\right)\right]^{-1}. \quad (5)$$

Here, ω is the angular frequency and τ is the time delay. The duration of a pulse described by Eqns (3)–(5) is $\Delta t_p = 1.278T_0$ and is related to the ACT width $\Delta\tau_a$ by $\Delta t_p = \Delta\tau_a/1.57$. As follows from Fig. 9, the above functions adequately represent the measured spectra and pulse intensity ACTs, which is particularly clear when comparison is made with the best fit Gaussian.

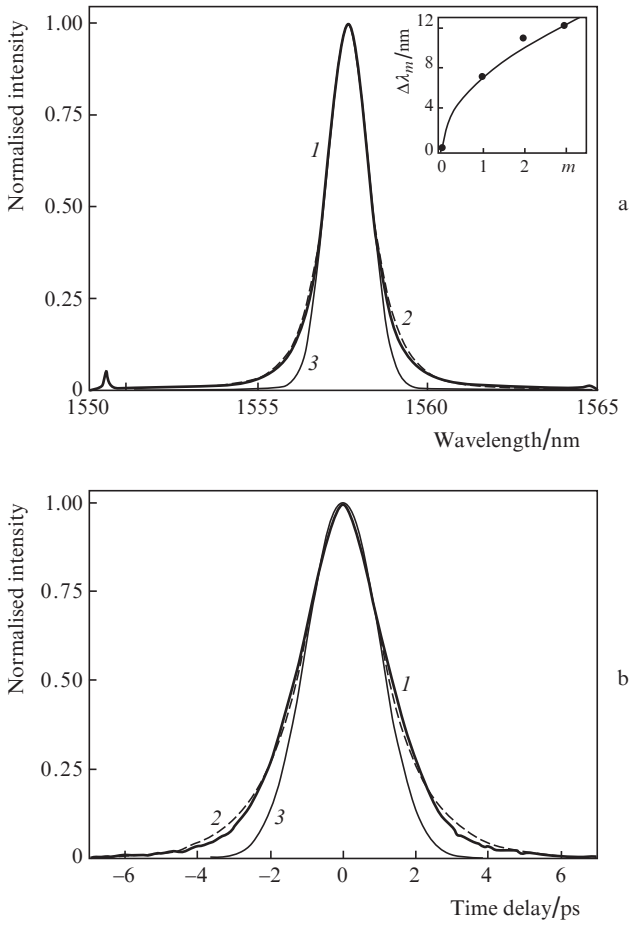

Figure 9. (a) Emission spectrum and (b) fitting of the measured pulse intensity ACT of the laser containing sample 3 at $D_2 = +0.129$ ps^2: (*1*) measured ACT and spectrum, (*2*) curves obtained using Eqns (4) and (5), (*3*) Gaussian. Inset: wavelength shift of the sideband vs. its order.

The most striking feature of the pulses under consideration is that their time–bandwidth product is $C = 0.22$ [20]. Pulses corresponding to curves (*3*) in Figs 8 and 9 have $C = 0.31$, which means that they are slightly chirped. An increase in their energy leads not only to an increase in their duration but also to a reduction in the parameter C (to 0.277) for pulses of 2.7-ps duration, corresponding to curve (*4*) in Fig. 8. At lower D_2 values, the parameter C varies only slightly, and an increase in GVD leads to the generation of even more bandwidth-limited pulses with smaller chirp ($C = 0.26$ at $D_2 = +0.194$ ps^2; see Fig. 3). Thus, we conclude that we observed

nearly bandwidth-limited pulses at an appreciable normal cavity GVD.

Even though the emission spectra of the lasers containing (opaque) films 1 and 2 (Fig. 8) have weaker sidebands in comparison with sample 3, they are best fitted by the same function of the form (4), whereas the pulse intensity ACT is best fitted by function (5), as illustrated in Fig. 10. Therefore, the observed laser operation mode in the normal GVD region is essentially independent of the properties of the saturable absorber, gain and cavity loss and is only determined by the mutual influence of nonlinearity and dispersion during pulse propagation (like in the case of fundamental soliton generation).

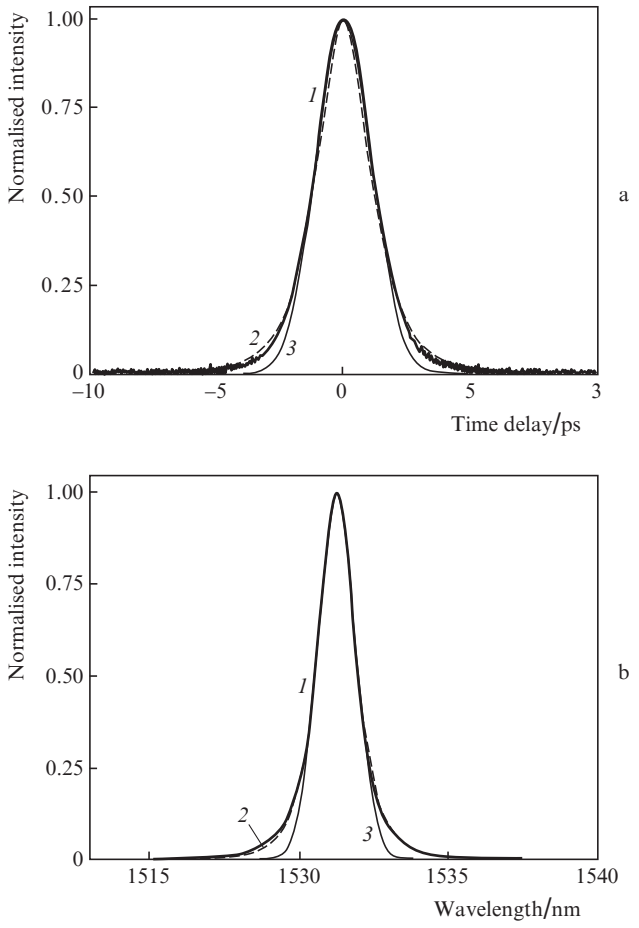

Figure 10. (a) Fitting of the measured pulse intensity ACT and (b) emission spectrum of the laser containing sample 2 at $D_2 = +0.129$ ps^2: (*1*) measured ACT and spectrum, (*2*) curves obtained using Eqns (4) and (5), (*3*) Gaussian.

We believe that the sidebands in the observed spectra are attributable to the effect of degenerate four-wave mixing (FWM) in the highly nonlinear GeO_2/SiO_2 fibre [22]. The wavelength shift of the sideband, $\Delta\lambda_m$, is related to its order m (Fig. 9, inset) by

$$\Delta\lambda_m = \pm\frac{\lambda_c^2}{c}\left[\frac{m}{2\pi L_{coh}|\beta_2|}\right]^{1/2}, \qquad (6)$$

where λ_c is the centre wavelength of the laser and L_{coh} is the coherence length, over which the FWM phase-matching condition should be fulfilled. The coherence length at $D_2 = +0.129$ ps^2 (Fig. 9) was estimated at 0.92 m, which correlates well with the GeO_2/SiO_2 fibre length (0.9 m).

The atypical spectral shape, the presence of sidebands and the nonstandard time–bandwidth product attest to the generation of a new type of pulse, different from fundamental solitons and positively chirped Gaussian pulses. At the same time, the presence of sidebands, which are similar to Kelly peaks, characteristic of soliton lasers, and the fact that the pulse energy is directly proportional to the pulse duration lead us to view the observed pulses as inversely modified solitons [25]. Necessary conditions for their propagation are high normal dispersion and nonlinearity in the cavity.

4. Conclusions

We have demonstrated an all-fibre erbium-doped ring laser with intracavity GVD management, passively mode-locked by SWCNTs dispersed in carboxymethylcellulose-based polymer films.

Experimental data are presented on the effect of cavity GVD and absorption in SWCNT-containing films on the key laser characteristics. At anomalous cavity GVD, the laser generated soliton-like pulses of duration 0.67 to 1.2 ps, depending on the energy and characteristics of the saturable absorber. At a near-zero net cavity GVD, we observed the generation of linearly chirped pulses up to 13 ps in duration, with an almost rectangular spectrum. The largest emission bandwidth was 8.4 nm, with a centre wavelength near 1560 nm and the highest average power of 10.5 mW. It is worth noting that this laser operation mode is optimal for subsequent pulse amplification and compression.

We have demonstrated the generation of a new type of almost transform-limited pulse – an inversely modified soliton – at normal cavity GVD and in the presence of highly nonlinear fibre. The shortest duration of such pulses was about 1.5 ps, with a spectral width of about 1.5 nm and an average output power of 2.9 mW.

Acknowledgements. We thank M.M. Bubnov, M.E. Likhachev and V.M. Mashinsky for providing the optical fibres. We are deeply grateful to B.L. Davydov for providing the fibre coupler and to A.K. Senatorov, A.F. Kosolapov and M.S. Astapovich for measuring the GVD of the fibres.

This work was supported by the Russian Academy of Sciences through the Fundamental Issues in the Technology of Nanostructures and Nanomaterials Programme.

References

1. Fermann M.E. *IEEE J. Quantum Electron.*, **15**, 191 (2009).
2. Nelson L.E., Jones D.J., Tamura K., Haus H.A., Ippen E.P. *Appl. Phys. B*, **65**, 277 (1997).
3. Turitsyn S.K., Shapiro E.G., Medvedev S.B., Fedoruk M.P., Mezentsev V.K. *Opt. Telecommun.*, **4**, 145 (2003).
4. Im J.H., Choi S.Y., Rotermund F., Yeom D.-I. *Opt. Express*, **18**, 22141 (2010).
5. Nishizawa N., Nozaki Y., Itoga E., Kataura H., Sakakibara Y. *Opt. Express*, **19**, 21874 (2011).
6. Guina M., Xiang N., Okhotnikov O.G. *Appl. Phys. B*, **74**, S193 (2002).
7. Set S.Y., Yaguchi H., Tanaka Y., Jablonski M., Sakakibara Y., Rozhin A., Tokumoto M., Kataura H., Achiba Y., Kikuchi K. *Book of abstracts OFC'03* (USA, OSA, PD44, 2003).
8. Tatsuura S., Furuki M., Sato Y., Iwasa I., Tian M., Mitsu H. *Adv. Mater.*, **15**, 534 (2003).

9. Set Sze Y., Yaguchi H., Tanaka Y., Jablonski M. *IEEE J. Sel. Top. Quantum Electron*., **10**, 137 (2004).
10. Kataura H., Kumazawa Y., Maniwa Y., Umezu I., Suzuki S., Ohtsuka Y., Achiba Y. *Synth. Met.*, **103**, 2555 (1999).
11. Saito R. et al. *Appl. Phys. Lett*., **60**, 2204 (1992).
12. Tausenev A.V., Obraztsova E.D., Lobach A.S., Konov V.I., Konyashchenko A.V., Kryukov P.G., Dianov E.M. *Kvantovaya Elektron*., **37**, 847 (2007) [*Quantum Electron*., **37**, 847 (2007)].
13. Dianov E.M., Mashinsky V.M. *J. Lightwave Technol.*, **23**, 3500 (2005).
14. Journet C. *Nature*, **388**, 756 (1997).
15. Obraztsova E.D. et al. *Nanostruct. Mater.*, **12**, 567 (1999).
16. Chernov A.I. et al. *Phys. Status Solidi B*, **224**, 4231 (2007).
17. Tausenev A.V. et al. *Kvantovaya Elektron*., **37**, 205 (2007) [*Quantum Electron*., **37**, 205 (2007)].
18. Tausenev et al. *Appl. Phys. Lett.*, **92**, 171113 (2008).
19. Digonnet M.J.E. *Rare-Earth-Doped Fiber Lasers and Amplifiers* (New York: Marcel Dekker, 2001).
20. Diels J.-C.M., Fontaine J.J., McMichael I.C., Simoni F. *Appl. Opt*., **24**, 1270 (1985).
21. Kelly S.M. *Electron. Lett*., **28**, 806 (1992).
22. Agrawal G.P. *Applications of Nonlinear Fiber Optics* (San Diego: Academ. Press, 2001).
23. Bale B.G., Boscolo S., Turitsyn S.K. *Opt. Lett.*, **34**, 3286 (2009).
24. Ippen E.P. *Appl. Phys. B*, **58**, 159 (1994).
25. Chernysheva M.A., Krylov A.A., Ogleznev A.A., Arutyunyan N.R., Pozharov A.S., Obraztsova E.D., Dianov E.M. *Opt. Express*, **20**, 23994 (2012).